

# Developable Surface Segmentation For CAD Models

Zheng Zeng  
KLMM,AMSS,CAS,UCAS  
Beijing, China  
zengzheng14@amss.ac.cn

Xiaohong Jia  
KLMM,AMSS,CAS,UCAS  
Beijing, China  
xhjia@ucas.ac.cn

Liyong Shen  
UCAS  
Beijing, China  
lyshen@ucas.ac.cn

Pengbo Bo  
HIT  
Harbin, China  
bob\_pengbo@163.com

## ABSTRACT

We present a novel method to segment CAD models into developable patches by detecting curve-like features on Gauss images of the corresponding patches. A region-growing approach is employed to detect planar and curved developable patches. The Gauss image of each segmented patch is constrained to be curve-like via principal component analysis and Pearson correlation analysis. Experimental results demonstrate that our approach generates nice results on CAD models with all kinds of developable surfaces.

## KEYWORDS

Developable surface, Segmentation, CAD models

### ACM Reference Format:

Zheng Zeng, Xiaohong Jia, Liyong Shen, and Pengbo Bo. 2021. Developable Surface Segmentation For CAD Models. In *Special Interest Group on Computer Graphics and Interactive Techniques Conference Posters (SIGGRAPH '21 Posters)*, August 09-13, 2021. ACM, New York, NY, USA, 2 pages. <https://doi.org/10.1145/3450618.3469167>

## 1 INTRODUCTION

Developable surfaces are widely used in industrial manufacturing and architectural modeling. Current methods for developable surfaces design generally require a clean segmentation setup which segments a mesh into developable strips and planes [Solomon et al. 2012; Tang et al. 2016], such as a segmentation in Fig. 1.

Existing approaches for developable segmentation cannot guarantee a nice result on CAD models. Julius et al. [2005] segment the mesh by detecting a subclass of developable surfaces. [Yamauchi et al. 2005] generate disk-like patches, but non-disk patches such as cylinders appear in CAD models quite often. Sharp creases in CAD models can also be a problem in recent research [Ion et al. 2020].

In this poster, we propose a novel method for extracting developable patches from CAD models by detecting curve-like features on Gauss images of each patch. The advantage of having curve-like Gauss image on each patch is that the patch can be fitted by a developable strip, which can be used in downstream applications directly. An example of our approach is shown in Fig. 1.

## 2 PRELIMINARIES

*Smooth developable surfaces.* Differential geometry offers profound insights into the nature of smooth developable surfaces.

Permission to make digital or hard copies of part or all of this work for personal or classroom use is granted without fee provided that copies are not made or distributed for profit or commercial advantage and that copies bear this notice and the full citation on the first page. Copyrights for third-party components of this work must be honored. For all other uses, contact the owner/author(s).  
SIGGRAPH '21 Posters, August 09-13, 2021, Virtual Event, USA  
© 2021 Copyright held by the owner/author(s).  
ACM ISBN 978-1-4503-8371-4/21/08.  
<https://doi.org/10.1145/3450618.3469167>

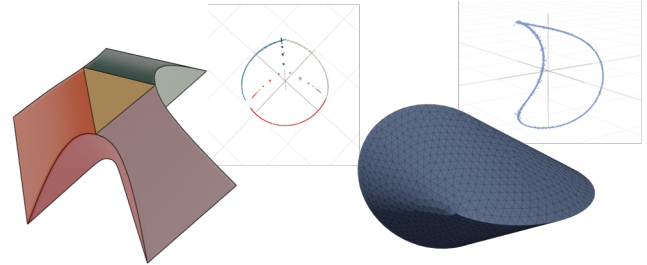


Figure 1: Left: Our result on bridge model and its Gauss image. The model is segmented into seven developable patches which include a yellow plane triangle at top and six developable strips. Right: Our result on oloid model and its Gauss image. The model has one developable surface.

Smooth developable surfaces are locally isometric to planes, such isometry can be characterized by vanishing Gaussian curvature at all points. This definition is advantageous to recognizing a developable surface rather than generating one. An efficient way to generate developable surfaces is to draw them as torsal ruled surfaces. A torsal ruled surface  $S$  can be parameterized by  $S(u, v) = \lambda(u) + v\gamma(u)$ ,  $(\lambda'(u) \times \gamma(u)) \cdot \gamma'(u) = 0$ , where  $\lambda(u)$  is a curve in  $\mathbb{R}^3$  called directrix,  $\gamma(u)$  is a nonvanishing vector field along  $\lambda(u)$  specifying the direction of rulings, and the equation on the right constrains Gaussian curvature to be zero. Furthermore, the normals of the torsal ruled surface is given by  $n(u) = \frac{\lambda'(u) \times \gamma(u)}{\|\lambda'(u) \times \gamma(u)\|}$ . Since  $n(u)$  is single parameterized, it forms a single curve in the sphere.

*Gauss map of triangle meshes.* Given a triangle mesh  $M = \{V, F\}$  with vertex set  $V$  and face set  $F$ , the Gauss map  $G$  of  $M$  maps each face  $f_i$  to face normal  $n_i$ . The Gauss image for  $M$  is  $N = \{n_i | i = 1 \dots m\}$ . Our goal is to find curve-like point clouds from  $N$ .

*Linearity.* To find curve-like point clouds, we measure the linearity locally. In statistics, the Pearson correlation coefficient measures the linear correlation between two sets of data. [Lee 2000] use this coefficient to measure the linearity of a point set in  $\mathbb{R}^3$ . For a point set  $N$ , map it to 2d plane such that the principle direction of the result point set  $P$  coincides with the identity line, then the Pearson correlation coefficient of  $P$  measures the linearity  $L(N)$  of  $N$ . If  $N$  forms a line,  $L(N)$  would be close to 1. If  $N$  is distributed randomly,  $L(N)$  would be close to 0.

## 3 METHODOLOGY

Our algorithm processes regular triangle or quadrilateral meshes. The workflow is shown in Fig. 2. We use a region-growing method to detect planes and developable patches. A seed face used for growing is chosen from regions as flat as possible. During growing

iteration, we constrain the neighbor of each face in the patch has a curve-like Gauss image. We say a face  $f_j \in F$  belongs to the  $i$ -neighbor  $U_k^i$  of  $f_k \in F$  if there exists at most  $i + 1$  faces  $\bar{f}_1 = f_k, \bar{f}_2, \dots, \bar{f}_{i+1} = f_j$  in  $F$  such that  $\bar{f}_l$  and  $\bar{f}_{l+1}$  ( $l = 1 \dots i$ ) have common edges. The principle value and principle direction of a face set  $I_k$  is the maximum principle value and the corresponding principle vector of  $\{n_j - \bar{n}_k | n_j \in G(I_k)\}$ ,  $\bar{n}_k$  is the mass center of  $G(I_k)$ . The principle direction and the principle value of a face  $f_k$  is the principle direction and the principle value of  $U_k^2$ .

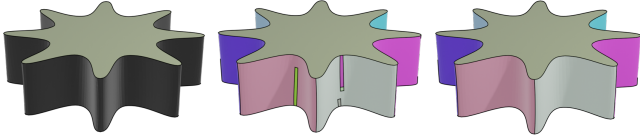


**Figure 2: Workflow of our algorithm. Left: plane detection with  $a_p = 0.001$ ; Middle: developable surface segmentation with  $L = 0.94, C = 0.9$  generates 19 patches; Right: segmentation clean generates 10 patches.**

*Plane Detection.* Our method first detects planar regions  $M_p$  of  $M$ . Faces with principle values less than  $a_p$  can be used as seeds. We grow a seed  $f_k$  by iteratively adding neighbor faces into segments  $I_k$  and constraining the principle value of  $G(I_k)$  to be less than  $a_p$ .

*Developable Surface Segmentation.* This stage detects non-planar developable pieces of  $M \setminus M_p$ . The seed face set  $S_k = \{f_k, f_1, f_2\}$  in this step is given by the face  $f_k$  with minimum principle value and  $f_1, f_2$  are chosen from  $U_k^1$  such that the principle direction of  $S_k$  is closest to the principle direction of  $f_k$ . During the growing process, we constrain the linearity  $l_j = L(G(U_{f_j}^2 \cap S_k))$  and tangent direction consistency  $c_j$  to be less than  $L$  and  $C$  respectively for each candidate face  $f_j$ . To guarantee  $G(S_k)$  can be approximated by a curve without branch road, we compute the tangent direction consistency  $c_j = \max_{t_l \in T_j} |t_l \cdot t_j|$ , where  $T_j$  is the set of principle directions for faces in  $U_l^2 \cap S_k$  and  $t_j$  is the principle direction of  $f_j$ .

*Segmentation Clean.* Our algorithm may produce small patches due to noise on the mesh or improper custom parameter choice (see figure2 middle). We clean these small patches by deleting patches with face number small than  $s$  and grow remaining patches with relaxed parameters  $a_p, L$  and  $C$ . Both  $L$  and  $C$  disallow rapid changes on the normal of a small region. In order to group the equator side of the gears model together,  $L$  and  $C$  need to be reduced to 0.6.

## 4 EXPERIMENTAL RESULTS

To find appropriate  $L$  and  $C$ , we segment gears model using different parameters. See table 1 for the number of segment patches. When  $C$  is larger than 0.99,  $L$  hardly effects the result. When  $C$  is reduced to 0.8, our algorithm starts to group side faces into one patch and generate small patches along the gear corner. When  $C$  is between 0.94 and 0.9, the behavior of our algorithm is more predictable since patch number will reduce as  $L$  reduce. When  $L$  is between 0.8 to 0.94, the results are cleaner. Thus  $L$  and  $C$  can be chosen between  $[0.8, 0.94]$  and  $[0.94, 0.9]$  respectively. All results generated within this range will be cleaned into 10 patches after segmentation clean.

**Table 1: patch number of developable surface segmentation for gears model using different parameters**

	C=0.99	C=0.94	C=0.9	C=0.8
L=0.99	103	64	59	60
L=0.94	101	64	19	12
L=0.9	101	33	18	20
L=0.8	101	33	17	18

Our method generates promising results for CAD models (see Fig. 3). In these examples,  $a_p$  is set to 0.001 for plane detection. Both  $L$  and  $C$  is set to 0.9 for developable surface detection. During the clean process,  $a_p$  is relaxed to 0.02,  $L$  and  $C$  is relaxed to 0.7. Notice that a developable patch will not expand into non-developable patch. The shape of the green patch in the first modle in Fig. 3 is like part of a bending tube, which is non-developable, and it will not be merged with neighboring developable patches. Our algorithm also works on developable surfaces that are not uni-axial conics such as oloids in Fig. 1 on the right.

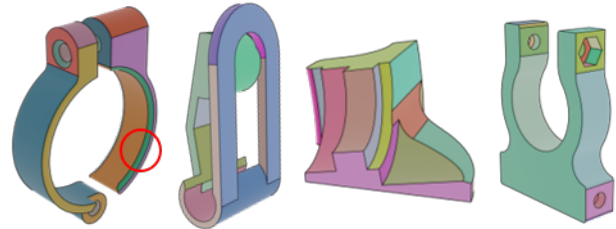


**Figure 3: More results of our proposed method.**

## 5 CONCLUSION AND FUTURE WORK

We propose an efficient method to segment CAD models into developable surfaces. Our results can be used as a setup to fit a model with developable surfaces. For noisy meshes, our method may not generate smooth boundaries. In future work, we will fit these segments with smooth developable surfaces and deal with the boundary.

## ACKNOWLEDGMENTS

This work was partially supported by the Beijing Natural Science Foundation (No. Z190004) and the National Natural Science Foundation of China (Nos. 12022117, 61872354 and 62072139).

## REFERENCES

- Alexandra Ion, Michael Rabinovich, Philipp Herholz, and Olga Sorkine-Hornung. 2020. Shape Approximation by Developable Wrapping. *ACM Trans. Graph.* 39, 6, Article 200 (Nov. 2020), 12 pages.
- Dan Julius, Vladislav Kraevoy, and Alla Sheffer. 2005. D-Charts: Quasi-Developable Mesh Segmentation. *Computer Graphics Forum* 24, 3 (2005), 581–590.
- In-Kwon Lee. 2000. Curve reconstruction from unorganized points. *Comp. Aided Geom. Design* 17, 2 (2000), 161–177.
- Justin Solomon, Etienne Vouga, Max Wardetzky, and Eitan Grinspun. 2012. Flexible Developable Surfaces. *Computer Graphics Forum* 31, 5 (2012), 1567–1576.
- Chengcheng Tang, Pengbo Bo, Johannes Wallner, and Helmut Pottmann. 2016. Interactive Design of Developable Surfaces. *ACM Transactions on Graphics* 35, 2, Article 12 (Jan. 2016), 12 pages. <https://doi.org/10.1145/2832906>
- Hitoshi Yamauchi, Stefan Gumhold, Rhaleb Zayer, and Hans-Peter Seidel. 2005. Mesh segmentation driven by Gaussian curvature. *The Visual Computer* 21, 8 (2005), 659–668.